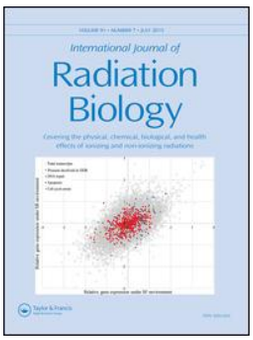

International Journal of Radiation Biology

ISSN: 0955-3002 (Print) 1362-3095 (Online) Journal homepage: http://www.tandfonline.com/loi/irab20

Increased radiotoxicity in two cancerous cell lines irradiated by low and high energy photons in the presence of thio-glucose bound gold nanoparticles

Shokouhozaman Soleymanifard, Atefeh Rostami, Seyed Amir Aledavood, Maryam M. Matin & Ameneh Sazgarnia

To cite this article: Shokouhozaman Soleymanifard, Atefeh Rostami, Seyed Amir Aledavood, Maryam M. Matin & Ameneh Sazgarnia (2017) Increased radiotoxicity in two cancerous cell lines irradiated by low and high energy photons in the presence of thio-glucose bound gold nanoparticles, International Journal of Radiation Biology, 93:4, 407-415, DOI: 10.1080/09553002.2017.1268282

To link to this article: http://dx.doi.org/10.1080/09553002.2017.1268282

Accepted author version posted online: 06 Dec 2016.
Published online: 12 Jan 2017.

INTERNATIONAL JOURNAL OF RADIATION BIOLOGY, 2017
VOL. 93, NO. 4, 407–415
http://dx.doi.org/10.1080/09553002.2017.1268282

Taylor & Francis
Taylor & Francis Group

ORIGINAL ARTICLE

Increased radiotoxicity in two cancerous cell lines irradiated by low and high energy photons in the presence of thio-glucose bound gold nanoparticles

Shokouhozaman Soleymanifard[a], Atefeh Rostami[b], Seyed Amir Aledavood[c], Maryam M. Matin[d] and Ameneh Sazgarnia[a]

[a]Medical Physics Research Center, Mashhad University of Medical Sciences, Mashhad, Iran; [b]Department of Medical Physics, School of Medicine, Mashhad University of Medical Sciences, Mashhad, Iran; [c]Cancer Research Center, Faculty of Medicine, Mashhad University of Medical Sciences, Mashhad, Iran; [d]Department of Biology, School of Sciences, Ferdowsi University, Mashhad, Iran

ABSTRACT

Purpose: Gold nanoparticles modified by thio-glucose are believed to increase the toxicity of radiotherapy in human malignant cells. We report the effect of thio-glucose bound gold nanoparticles (Glu-G nanoparticles), 16 nm in size, on two human lung (QU-DB) and breast (MCF7) cancer cell lines combined with kilo and megavoltage X-rays.

Materials and methods: The shape and surface characteristics, the size distribution and light absorption spectrum of the prepared nanoparticles were measured by transmission electron microscopy, dynamic light scattering, and ultraviolet-visible spectrophotometry, respectively. The cell uptake was assayed using the atomic absorption spectrometry. Mitochondrial activity, colony formation, and comet assays were applied to assess and compare the enhanced radiotoxicity of 100 KV and 6 MV X-rays, when combined with Glu-G nanoparticles.

Results: Glu-G nanoparticles had no significant toxicity for MCF7 and QU-DB cells up to 100 micromolar concentration. Compared to radiation alone, the intracellular uptake of Glu-G nanoparticles resulted in increased inhibition of cell proliferation by 64.1% and 38.7% for MCF7 cells, and 64.4% and 32.4% for QU-DB cells by 100 kVp and 6 MV X-rays, respectively. Comet assay confirmed an increase of DNA damage as a result of combination of 6 MV photons with Glu-G nanoparticles.

Conclusion: Glu-G nanoparticles have remarkable potential for enhancing radiotoxicity of both low and high energy photons in MCF7 and QU-DB cells.

ARTICLE HISTORY
Received 23 July 2015
Revised 13 November 2016
Accepted 21 November 2016

KEYWORDS
Gold nanoparticles; MCF7 cell line; QU-DB cell line; comet assay; thio-glucose

Introduction

Surgery, chemotherapy, and radiation therapy are three major treatment modalities for cancer. Among them, radiation therapy has the advantage of non-invasiveness, and is extensively employed to treat approximately all solid tumor types (Kobayashi et al. 2010). In radiotherapy, a therapeutic mechanism is needed in order to enhance the therapeutic ratio (increasing cancer cell killing, while minimizing cytotoxicity to surrounding tissues). Development of modern radiotherapy techniques in order to limit radiation to tumor and employment of heavy particles instead of X-rays are examples of efforts made to achieve this goal. The application of radiosensitizers is another way to enhance the therapeutic ratio. Elements such as silicon, platinum and gold, which have been used as contrast agents to overcome the lack of soft tissue differentiation in medical imaging, have been investigated with the aim of increasing the radiosensitivity of cancerous cells (Bhattacharyya et al. 2011). Besides, tumor-specific nanoparticles have recently been used in radiotherapy to improve toxicity in tumors, while excluding normal tissues (Hainfeld et al. 2008).

Due to the biocompatibility and relatively non-toxic nature among all nanoparticles, gold has been widely used (Bhattacharyya et al. 2011). Recently, Bhattacharya et al. demonstrated that gold nanoparticles can be used as active agents to interfere directly with cellular processes and induce anti-angiogenic and antitumor effects (Bhattacharyya et al. 2011). Enhancement of radiation effects by gold nanoparticles depends on the number of particles taken up by target cells. Cellular uptake of gold nanoparticles depends on the cell type and certainly the size and surface coating of nanoparticles (Chithrani et al. 2006; Cho et al. 2010; Malugin & Ghandehari 2010; Trono et al. 2011). Furthermore, images provided by positron emission tomography have confirmed that most malignant tumors absorb glucose more effectively than normal cells (Kong et al. 2008). This unique metabolic characteristic of malignant cells can be used to design nanoparticles for targeted delivery. Gold nanoparticles bounded to glucose have been studied extensively. The reported results indicate that glucose-capped gold nanoparticles, which are designed based on cancer cell metabolism, can be selectively taken up by cancerous cells and accumulate in the cytoplasm (Kong et al. 2008; Zhang et al. 2008; Wang et al. 2013, 2015). Exposure to thio-glucose bound gold nanoparticles (Glu-G nanoparticles) has resulted in a three times increase in particle absorption compared to that of

CONTACT Ameneh Sazgarnia sazgarniaa@mums.ac.ir Medical Physics Research Center, Department of Medical Physics, Faculty of Medicine, Pardis, Vakil Abad Boulevard, Mashhad 9188857468, Iran

naked gold nanoparticles (Zhang et al. 2008). Cytoplasmic intracellular uptake of neutral gold nanoparticles and Glu-G nanoparticles resulted in a growth inhibition by (30.6 ± 3.3)% and (46.0 ± 3.9)% respectively; while for radiation alone, the same figure was (15.8 ± 2.8)% (Zhang et al. 2008). In the study carried out by Kong et al., Glu-G nanoparticles and cysteamine-capped gold nanoparticles with the diameter of 10.8 nm were used to enhance radio cytotoxicity of MCF7 cells. With 10 Gy of 200 kVp X-rays, cytotoxicity increased up to 63.5% for Glu-G nanoparticles and 31.7% for cysteamine-capped gold nanoparticles. It is worth noting that Glu-G nanoparticles enter the cell cytoplasm through endocytosis, whereas cysteamine-capped gold nanoparticles are strongly positive, and just bind onto the cell surface. This finding indicates that the location of gold nanoparticles in the cells is an important factor in the increased rate of radiation cytotoxicity (Kong et al. 2008).

The effectiveness of heavy element nanoparticles, when combined with low energy photons, has been established by several studies. This effect is attributed to the enhanced radiation dose as a result of radiation interaction with heavy elements in the nanoparticles' structure through the photoelectric effect (Rahman et al. 2009; Butterworth et al. 2010). On the other hand, megavoltage photons are far more common in radiation therapy, and recent studies have focused on the effectiveness of nanoparticles on high energy photons' cytotoxicity. Meanwhile, due to the predomination of the Compton effect for high energy photons, dose enhancement is not expected. Nevertheless, results of several studies have revealed that nanoparticles combined with high energy photons increase radiation cytotoxicity. Geng et al. compared 90 kVp and 6 MV energies. The intracellular uptake of Glu-G nanoparticles resulted in increased inhibition of cell proliferation by 30.5% for 90 kVp and 26.9% for 6 MV (Geng et al. 2011). Wang et al. studied the effect of gold nanoparticles, 13 nm in size, combined with megavoltage X-rays. They demonstrated the occurrence of significant radiosensitization in a lung cancer cell line with a sensitivity enhancement ratio (SER) of 1.5 (Wang et al. 2013).

The present study aimed to survey whether the effectiveness of Glu-G nanoparticles on high energy photon cytotoxicity can be confirmed. Thus, human lung (QU-DB) and breast (MCF7) cancer cell lines were treated with Glu-G nanoparticles, and were then irradiated with 100 kVp and 6 MV X-rays. Afterwards, in order to compare their enhanced cytotoxicity, 3-[4, 5-dimethylthiazol-2-yl]-2, 5-diphenyltetrazolium bromide (MTT) cellular proliferation and colony assays were applied. To confirm the correctness of MTT and colony assays, the comet assay was performed for the cells irradiated with 6 MV X-rays.

Materials and methods

Synthesis of Glu-G nanoparticles

Gold (III) chloride tri-hydrate ($HAuCl_4{\cdot}3H_2O$, G4022-1g) (Sigma-Aldrich, St. Louis, MO), 1-thio-β-D-glucose (Glu, T6375-1G) (Sigma-Aldrich), and Sodium borohydride ($NaBH_4$, 16940-66-2) (Sharlau, Barcelona, Spain) were used to synthesis Glu-G nanoparticles in three sub-steps: (i) 3.2 ml of deionized water was shaken with 0.03 g $HAuCl_4$; the solution was then added to 60 ml of deionized water in an ice bath under moderate stirring; (ii) The watery $NaBH_4$ (0.004 g in 4 ml deionized water) was added to the mixture prepared in the first step to act as a reducing agent and to obtain a naked gold nanoparticle solution; (iii) 12 ml of deionized water was added to 0.05 g 1-thio-β-D-glucose; this mixture was then added to the naked gold nanoparticle solution. Thio-glucose formed a covalent bond with the gold nanoparticles to form functionalized Glu-G nanoparticles. The Glu-G nanoparticles were dialyzed for 2 days and before using were centrifuged to remove naked gold nanoparticles.

Characterization of Glu-G nanoparticles

The mean size and the shape of the prepared nanoparticles were determined by transmission electron microscopy (TEM) (ZEISS, LEO 912 ab, Oberkochen, Germany); their size distribution was recorded by a dynamic light scattering (DLS) instrument (Malvern Instruments, Malvern, UK). The stability of Glu-G nanoparticles was checked using ultraviolet-visible (UV-Vis) spectrophotometry (UV-1700 Pharmaspect, Shimadsu, Japan) within a 200–800 nm range of Glu-G nanoparticle stock solutions. Atomic absorption spectrometry (AAS) (SpectrAA 220Z Atomic absorption, Midland, Canada) was used to measure the gold concentration in the gold nanoparticle solution.

Cell lines and culture conditions

Human breast adenocarcinoma cell line, MCF7, and human lung-cancer cell line, QU-DB, were purchased from Pasteur Institute in Tehran, Iran. The cells were cultured in Roswell Park Memorial Institute (RPMI) 1640 culture medium (GIBCO, Darmstadt, Germany) supplemented with 10% heat-inactivated fetal bovine serum (FBS) (GIBCO), streptomycin (Biosera, Kansas City, MO) (1 mg/ml), and penicillin (Biosera) (1000 units/ml), and then incubated at 37 °C in a humidified atmosphere with 5% CO_2.

Glu-G nanoparticles cytotoxicity

The cells were seeded in 96-well plates (Orange scientific, Braine-l'Alleud, Belgium) (1×10^4 cells/well). As soon as they attached to the wells' bottom, their media were replaced with FBS free culture media. Afterwards, they were treated with different concentrations of Glu-G nanoparticles (10, 20, 40, 50, 60, 70, 80, 90 and 100 μM). Two hours later, the cells were washed with phosphate buffered saline (PBS) and incubated in fresh medium containing 10% FBS for 24 h. Finally, by performing the MTT cellular proliferation test, their percentage viability was measured to determine the cytotoxicity of Glu-G nanoparticles.

Cell uptake of Glu-G nanoparticles

MCF7 and QU-DB cells were cultured in 25 cm^2 flasks (Orange scientific). When the cells reached 70% of

confluence, their culture media were replaced with FBS free culture media which contained 100 μM Glu-G nanoparticles. Incubation with Glu-G nanoparticles lasted for 2 h, and then the cells were collected and re-suspended into PBS for a final volume of 2 ml. A hemocytometer was used to determine the number of cells/ml. Afterwards, 3 ml HNO_3 (50%) was added to each sample to lyse the cells. The gold mass in the lysed solution was measured by AAS. The mass of one gold nanoparticle was calculated from the size of nanoparticles and the gold density (Evans 1994). The number of gold nanoparticles/cell was calculated based on the following equation:

$$\frac{\text{The number of GNP}}{\text{cell}} = \frac{\text{The mass of gold nanoparticles in the lysed solution}}{\text{The mass of one gold nanoparticle} \times \text{The number of cells}}$$

Experimental groups

Using MTT, colony, and comet assays, radiotoxicity was examined in four different groups of the cells as follows: control: the group which received no treatment; Glu-GNP: the group treated with Glu-G nanoparticles only; X-ray: the group treated with X-ray only; and Glu-GNP + X-ray: the group treated with both Glu-G nanoparticles and radiation.

Based on cell size, radiation dose, doubling time, and the time that cells need to be incubated for MTT and colony assays, the appropriate number of cells for placing in 96-well and six-well plates was determined. The cells were then cultured in 96-well plates (7×10^3 QU-DB cells/well, 2×10^3, 4×10^3, and 6×10^3 MCF7 cells/well), six-well plates (4×10^2 and 8×10^2 cells for MCF7, 2×10^3 and 3×10^3 cells for QU-DB control and irradiation groups, respectively), and 10 cm^2 flasks (5×10^5 cells). The plates and the flasks were prepared for MTT/colony assay and comet assay, respectively. On the next day, the cells which were planned to be treated with nanoparticles (Glu-GNP + X-ray), were exposed to 100 μM Glu-G nanoparticles for 2 h. They were then washed with PBS and fed with fresh culture medium. After 1 h, they were irradiated with 2 Gy of 6 MV/100 kVp X-rays. Irradiation was also simultaneously performed for the cells which were not treated with nanoparticles (X-ray group). One hour after irradiation, the cells were returned to the laboratory and manipulated for MTT, colony and comet assays. Two control groups (sham-irradiated cells with and without Glu-G nanoparticles) were handled in parallel with irradiated cells.

Irradiation

For irradiation with 6 MV X-rays a solid water slab (1.5 cm) was placed on a linear accelerator coach (Varian, Clinac 600, serial number: 475, CA), and the flasks/plates were placed on it. Then the flasks/plates were covered with 10 cm extra solid water slabs, and were irradiated when the gantry was at 180° position. Irradiation was performed with a dose-rate of 2.5 Gy/min at room temperature. For irradiation with 100 kVp X-rays the flasks/plates were placed on a $30 \times 30 \times 20$ cm^3 water phantom and covered with a 20×20 cm^2 applicator which was attached to a superficial X-ray unit (Philips, serial number: 2/625, Amsterdam, The Netherlands). Irradiation was performed at room temperature while dose-rate and source surface distance were 1.51 Gy/min and 30 cm, respectively.

MTT cellular proliferation test

The cells were cultured in 96-well plates. The rows of the plates dedicated to Glu-GNP + X-ray group were exposed to Glu-G nanoparticles for 2 h. They were then washed and fed with fresh culture medium. One hour later the whole plates containing both Glu-GNP + X-ray and X-ray groups were irradiated. Following irradiation, the plates containing MCF7 cells, in three groups, were incubated for 48, 72 and 144 h (plates with lower number of cells were incubated for a longer time). In addition, the plates containing QU-DB cells, in one group, were incubated for 48 h. Then the culture media of the wells were removed; 10 μl of MTT (3-[4,5-dimethylthiazol-2-yl]-2,5-diphenyltetrazolium bromide) (Sigma-Aldrich) and 100 μl of FBS free medium were added to individual wells and incubated for 4 h. Afterwards, the culture media in the wells were replaced with 200 μl of dimethyl sulfoxide (Sigma-Aldrich) and mixed for 10 min to dissolve the converted dye. Finally, using a multi-well scanning spectrophotometer (MIDSCI, Valley Park, MO), light absorbance was measured at 545 nm. The percentage of cell viability was measured in comparison to the control groups (sham-irradiated cells without Glu-G nanoparticles). Radiotoxicity enhancement was calculated as follows:

$$\text{Radio}-\text{toxicity enhancement} = \left(\frac{\%\ \text{cell viability with (X-ray)}}{-(\%\ \text{cell viability with (Glu}-\text{G nanoparticles} + \text{X-ray}))} \right) \times 100$$

Colony assay

The cells were incubated in 1:1 solution of 0.25% trypsin and 1 mM ethylenediaminetetraacetic acid (EDTA) (Sigma-Aldrich), and detached from the flasks. Following detachment, the cells were centrifuged and resuspended in fresh culture medium. Using a haemocytometer, the number of cells in 1 ml cell solution was determined, and then appropriate numbers of the cells were cultured in six-well plates (Orange scientific). The next day, the cells planned to be treated with nanoparticles (GNP + X-ray group) were exposed to gold nanoparticles for 2 h, and 1 h later they were irradiated. Irradiation was also performed for X-ray group. Following irradiation, the cells were incubated for 10–14 days (10 days for MCF7 and 14 days for QU-DB cells). To determine the cell survival fraction, the colonies attached to the flasks were fixed with pure methanol and stained with Giemsa. The colonies exceeding 50 cells were scored as representatives of surviving cells. Radiotoxicity enhancement was calculated employing the formula used for the MTT test.

Comet assay

The cells were incubated in 10 cm^2 flasks (Orange scientific). The next day the cells planned to be treated with nanoparticles (GNP + X-ray group) were exposed to gold nanoparticles for 2 h; 1 h later they were irradiated. Irradiation was performed for X-ray group as well. Comet assay, as follows, was performed 1 h after irradiation.

The alkaline comet assay was performed based on the method previously described by Singh et al., with some modifications (Singh et al. 1988; Mohammadi et al. 2012). One hour after irradiation, the cells were detached from the flasks, and some slides were covered with 1% normal melting point agarose (NMA) (Merck, Kenilworth, NJ). A total number of 1×10^4 cells were mixed with 75 µl 0.5% low melting point agarose (LMA) (Merck), and pipetted rapidly onto the prepared slides. To solidify the mixture, the slides were placed flat in the dark at 4 °C for 10 min. Then the slides were immersed in freshly prepared lysis buffer (2.5 M NaCl) (Sigma-Aldrich), 100 mM EDTA, 10 mM Tris-base with 1% Triton X-100, pH =10 (Sigma-Aldrich) and incubated for 1 h at 4 °C. Afterwards, the slides were removed from the lysis buffer and placed in a horizontal gel electrophoresis tank (CSL-COM20, Cleaver Scientific, Warwickshire, UK) filled with fresh cold denaturation buffer (300 mM NaOH) (Sharlau), 1 mM EDTA, pH =13). The slides were then left in the solution for 30 min, and electrophoresis was conducted in the same denaturation buffer using a voltage of 23 V and a current of 300 mA. Following electrophoresis, the slides were washed in Tris buffer (0.4 M Tris-HCl, pH =7.5 (Sigma-Aldrich) to neutralize the excess alkali. Finally, the slides were stained with ethidium bromide (20 µg/ml) (Sigma-Aldrich) for 5 min. The individual cells or comets were viewed and photographed using a fluorescent microscope (BX51, Olympus, Shinjuku, Tokyo, Japan) equipped with an ethidium bromide filter (excitation filter, 535 nm; emission filter, 610 nm) and a charge-coupled device camera (Olympus-DP71). The photographs were analyzed by Comet Score™ Freeware v1.5 software. DNA damage was quantified as an increase in tail moment, the amount of DNA (fluorescence) in the tail, and the distance between the means of the head and tail fluorescence distribution.

Statistical analysis

The data are presented as the mean of at least four independent experiments, replicated in three wells, for MTT and colony assays, respectively. SPSS version 21 was used to perform statistical analysis. Data distribution was normal, thus one-way analysis of variance (ANOVA) and Tukey's multiple comparison tests were performed to compare the groups at a significance level of $p < 0.05$.

Results

Characteristics of Glu-G nanoparticles

The average gold concentration of the gold nanoparticle solutions, which was measured by AAS, was 200 mg/l. Figure 1(A) shows the transmission electron microscopy (TEM) image of gold nanoparticles. Figure 1(B) shows the size distribution of gold nanoparticles measured by the DLS instrument. The mean diameter of the gold nanoparticles was 16 nm. The spectrum of Glu-G nanoparticles forming UV-Vis spectrophotometry is shown in Figure 1(C).

Cytotoxicity of Glu-G nanoparticles

The cells were incubated with different concentrations of Glu-G nanoparticles (10, 20, 30, 40, 50, 60, 70, 80, 90 and 100 µM), and the cytotoxicity of the nanoparticles was determined by the MTT test. Figure 2 shows the cell viability percentage of the two cell lines. The results indicated that Glu-G nanoparticles in either 10–100 µM concentrations did not induce remarkable cytotoxicity on MCF7 and QU-DB cells. Therefore, in the following experiments the maximum concentration (100 µM) was applied.

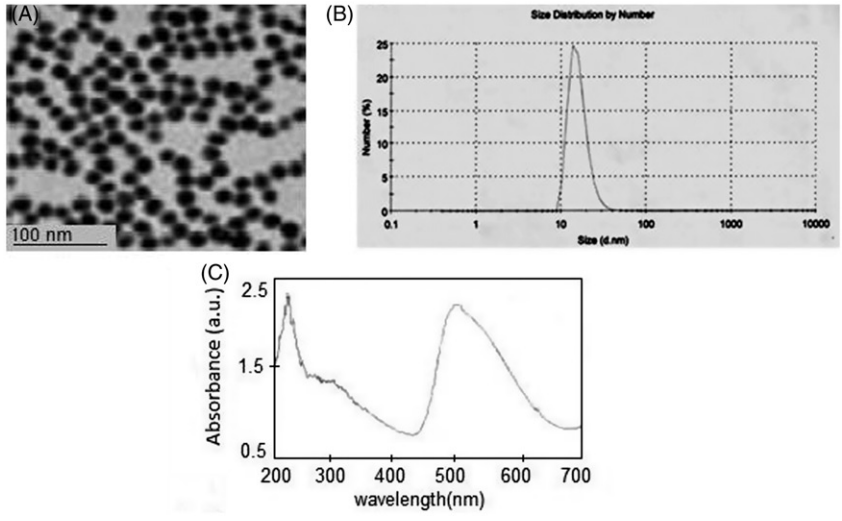

Figure 1. Characteristics of gold nanoparticles. (A) TEM image of gold nanoparticles; (B) the size distribution of gold nanoparticles measured by the DLS instrument; (C) light-absorbance diagram of Glu-G nanoparticles by UV-Vis spectrophotometry.

Uptake of Glu-G nanoparticles

The number of gold nanoparticles, which were taken up by MCF7 and QU-DB cells in cell lysis, was quantified on the basis of AAS. After the cells were exposed to 100 μM of Glu-G nanoparticles for 2 h, the average number of gold nanoparticles associated with each MCF7 and QU-DB cell line were 6.9×10^4/cell and 5.3×10^4/cell, respectively.

Radiotoxicity enhancement by Glu-G nanoparticles

The two groups of Glu-GNP and Glu-GNP + X-ray were treated with gold nanoparticles for 2 h. Both the treated and untreated cells were then irradiated with 100 kVp and 6 MV X-rays with a dose of 2 Gy. Induced cytotoxicity was assessed 48 h after irradiation with the MTT assay and after 10–14 days with the colony assay. The results of MTT assay and colony assay for 100 kVp are displayed in Figure 3(A) and (B), respectively. Statistical analyses, performed for both tests, indicated no significant difference between the two sham-irradiated groups (the control and Glu-GNP groups) ($p > 0.05$).

Figure 3(A) reveals that radiation alone (in X-ray group) decreased the cell viability of MCF7 and QU-DB cells up to 96.9% and 70.9%, respectively ($p > 0.05$ for MCF7 cells, and $p < 0.001$ for QU-DB cells compared to the controls). The cell viability of the cells having received both radiation and Glu-G nanoparticles treatment (Glu-GNP + X-ray group) decreased to 57.1% and 56.8% for MCF7 and QU-DB cells, respectively. The difference between Glu-GNP + X-ray group and X-ray group was statistically significant ($p < 0.001$). The enhancement of radiation toxicity as a result of applying Glu-G nanoparticles was equal to 40.9% and 19.8% for MCF7 and QU-DB cells, respectively.

The results of the clonogenic survival assay for 100 kVp are shown in Figure 3(B). The survival fraction of MCF7 and QU-DB X-ray groups were 46.2% and 52.6%, respectively ($p < 0.001$ compared to the control group), while the viability of Glu-GNP + X-rays groups of MCF7 and QU-DB cells decreased to 16.6% and 18.7%, respectively ($p < 0.001$ for both MCF7 and QU-DB cells compared to X-ray groups). Hence, as a result of applying Glu-G nanoparticles, radiotoxicity enhancement was equal to 69.2% and 64.4% for MCF7 and QU-DB cells, respectively.

Figure 3(A) shows that X-ray and control groups of MCF7 cells, in terms of cell viability and survival fraction, are statistically equal ($p > 0.05$). As it was unexpected, in addition to the first MTT test, which was performed after 48 h, the test was repeated twice, after 96 and 144 h (Figure 4). The results revealed that the cell viability of the X-ray group decreased gradually as the time passed ($p < 0.001$). However, in the Glu-GNP + X-ray group cell viability at 48 and 96 h was

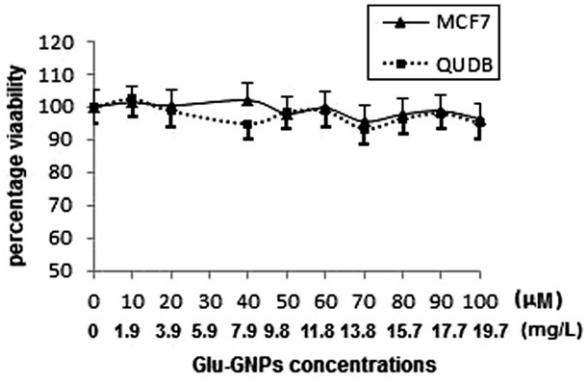

Figure 2. The results of the MTT test which was performed 24 hours after treatment the cells with different concentrations of Glu-G nanoparticles for 2 hours. Error bars indicate the standard deviation (SD) of four independent experiments.

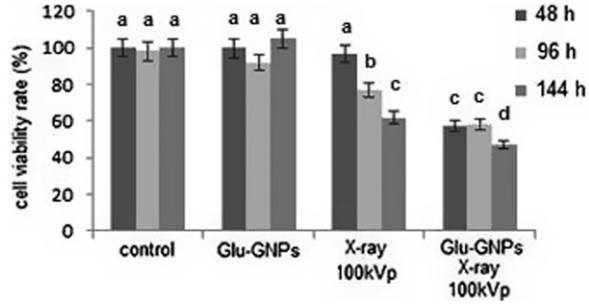

Figure 4. Results of the MTT test performed for MCF7 cells at different times after irradiation (48, 96 and 144 hours) with 100 kVp X-rays. Error bars indicate the standard deviation (SD) of four independent experiments. The groups are compared with one another. Two or three groups which have the same letters are not statistically different ($p > 0.05$), but every two groups which have different letters are statistically different ($p < 0.001$) compared to each other.

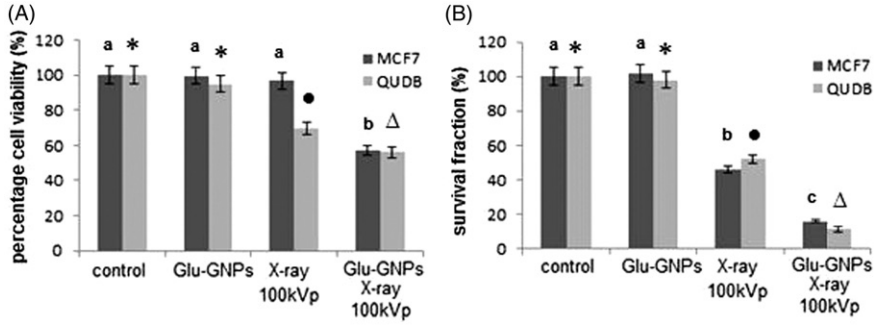

Figure 3. (A) Cell viability percentage, and (B) survival fraction of different groups exposed to 2 Gy of 100 kVp X-rays. Error bars indicate the standard deviation (SD) of four independent experiments. The columns of MCF7 cell line are compared with one another. Two or three columns which have the same letters are not statistically different ($p > 0.05$), but every two columns which have different letters are statistically different ($p < 0.001$) compared to each other. The columns of QU-DB cell line are compared with one another. Two or three columns which have the same shapes are not statistically different ($p > 0.05$), but every two columns which have different shapes are statistically different ($p < 0.001$) compared to each other.

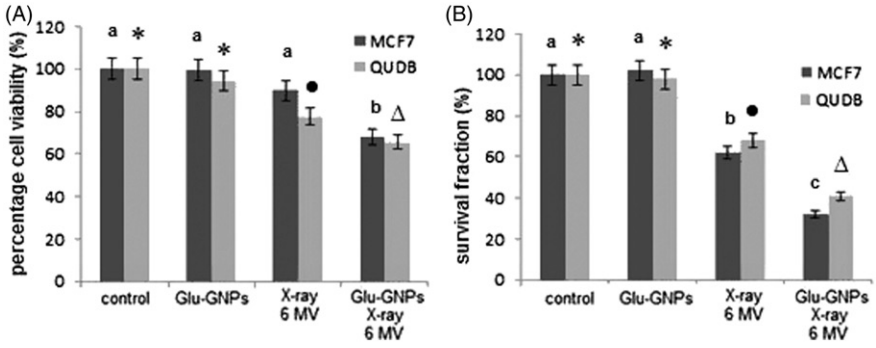

Figure 5. (A) Cell viability percentage, and (B) survival fraction of different groups exposed to 2 Gy of 6 MV X-rays. Error bars indicate the standard deviation (SD) of four independent experiments. The columns of MCF7 cell line are compared with one another. Two or three columns which have the same letters are not statistically different ($p > 0.05$), but every two columns which have different letters are statistically different ($p < 0.001$) compared to each other. The columns of QU-DB cell line are compared with one another. Two or three columns which have the same shapes are not statistically different ($p > 0.05$), but every two columns which have different shapes are statistically different ($p < 0.001$) compared to each other.

identical ($p = 1$), and decreased just after 144 h ($p < 0.004$). At each period that the experiment was performed, the results of X-ray and Glu-GNP + X-ray groups were statistically different ($p < 0.05$).

Figure 5(A) shows that radiation alone (in the 6 MV X-ray group) decreased the cell viability of MCF7 and QU-DB cells up to 89.8% and 77.6%, respectively ($p = 0.06$ for MCF7 cells and $p < 0.001$ for QU-DB cells compared to the control groups). The cell viability of the cells which received both radiation and Glu-G nanoparticles treatment (Glu-G nanoparticles +6 MV X-ray group) decreased to 67.9% and 65.4% for MCF7 and QU-DB cells, respectively. The difference between Glu-GNP + X-ray and X-ray groups was statistically significant ($p < 0.001$). The enhancement of radiation toxicity as a result of applying Glu-G nanoparticles was equal to 24.3% and 15.7% for MCF7 and QU-DB cells, respectively.

The results of the clonogenic survival assay for 6 MV photons are shown in Figure 5(B). The survival fraction of MCF7 and QU-DB X-ray groups were 62.9% and 68.5%, respectively ($p < 0.001$ compared to the control groups). The survival fraction of Glu-GNP + X-ray groups of MCF7 and QU-DB cells decreased to 38.2% and 46.3%, respectively ($p < 0.001$ compared to the X-ray group). As a result of applying Glu-G nanoparticles, radiotoxicity enhancement was equal to 39.3% and 32.4% for MCF7 and QU-DB cells, respectively.

To perform the comet assay, 100 cells of each group were analyzed in the comet score software. From each group one photograph of MCF7 and QU-DB cells is shown in Figure 6(A) and (B), respectively. Tail moment values are demonstrated in Figure 6(C). 6 MV X-rays induced a tail moment of 6.7 and 7.4 in MCF7 and QU-DB cells, respectively. Glu-G nanoparticles increased the tail moment of MCF7 and QU-DB cells up to 18.6 and 15.7, respectively. Statistical analysis revealed significant differences between X-ray and Glu-GNP + X-ray groups ($p < 0.001$) and also between these groups and the control groups for both MCF7 and QU-DB cells ($p < 0.001$).

Discussion

The findings of the present study demonstrated that Glu-G nanoparticles are able to increase radiosensitivity in both low and high energy photons; however, this was superior in low energy ones. Based on the results obtained by the colony assay, Glu-G nanoparticles increase the radiation sensitivity of MCF7 and QU-DB cells by 69.2% and 64.4%, respectively, for 100 kVp X-rays; while enhanced radiosensitivity for 6 MV X-rays was 39.3% in MCF7 cells and 32.4% in QU-DB cells. Moreover, the results of the comet assay, which were consistent with the results of both MTT and colony assays, confirmed that Glu-G nanoparticles increase radiosensitivity for 6 MV photons. Longer tail moment in Glu-GNP + X-ray group compared to the X-ray group may be attributed to either increased reactive oxygen species (ROS) formation or impaired capacity of the cells to repair DNA damage.

The radiosensitizing effects of metallic nanoparticles for low energy photons have been demonstrated by many researchers, and are attributed to the photoelectric effect which dominates other interactions between low energy radiations and materials. However, high energy photons interact with materials mainly through the Compton effect; hence, an enhanced absorbed dose by the nanoparticle is not expected. In addition, Monte Carlo studies did not show dose enhancement for megavoltage photons with gold nanoparticles (Van den Heuvel et al. 2010; Lechtman et al. 2011; Mesbahi and Jamali 2013; Pakravan et al. 2013). On the other hand, our results showed that Glu-G nanoparticles increase the effects of 6 MV photons. This observation is consistent with some other studies which indicate that metal nanoparticles enhance radiosensitivity for megavoltage photons as well as for kilo voltage X-rays (Geng et al. 2011; Wang et al. 2013, 2015). Since the amplified effect of megavoltage X-rays on cell death and increased DNA damage cannot be solely attributed to the high atomic number of metallic nanoparticles and consequently to the radiation dose, additional mechanisms must be taken into account. Some researchers have explained alternative underlying mechanisms of action. Turner et al. reported that metallic materials may arrest cells at the G2/M phase, the most radiosensitive cell cycle phase, and thus disproportionately increase the sensitivity of cancer cells for radiation (Turner et al. 2005). Geng et al. also explained that Glu-G nanoparticles induce radiosensitization by cell cycle regulation (Geng et al. 2011). Wang et al. demonstrated that Glu-G nanoparticles alone (without radiation) disrupt the balance between B-cell lymphoma 2 (Bcl-2) and

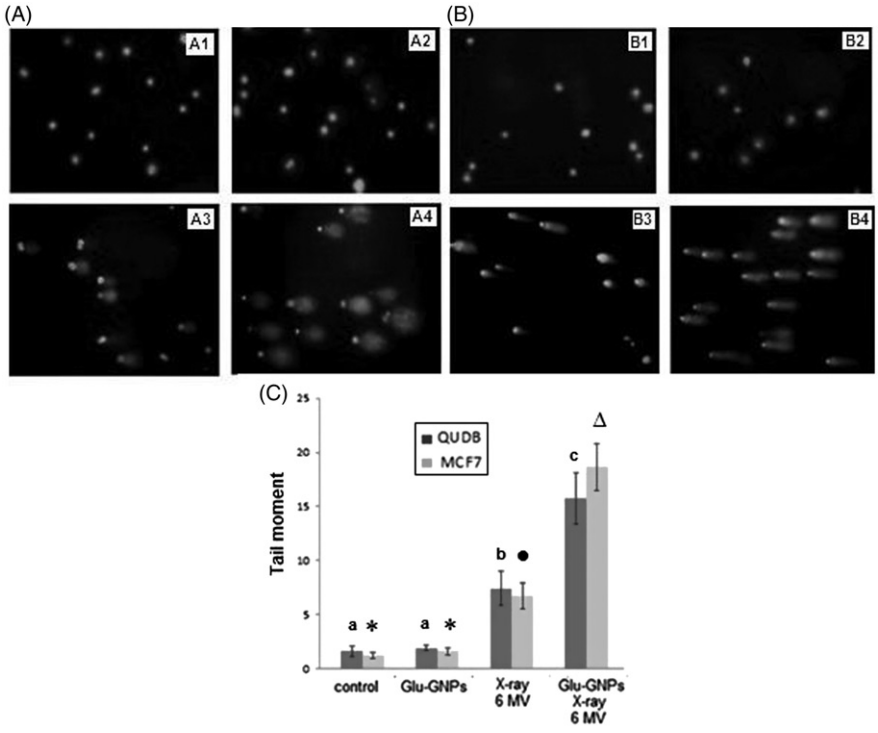

Figure 6. Comet images of MCF7 (photos A) and QU-DB cells (photos B) taken by a florescence microscope and the mean of determined tail moments of MCF7 and QU-DB cells in 6 MV X-rays experiment (C). (100 × (Total magnification) = 10 × (Objective) × 10 × (ocular eyepiece). (A1, B1) Control, (A2, B2) treated cells with nanoparticles, (A3, B3) irradiated cells with 6 MV X-ray radiation, (A4, B4) treated cells with nanoparticles and 6 MV X-ray radiation. Error bars in (C) indicate the standard deviation (SD) of four independent experiments. The groups, which have identical letters (for QU-DB cells), or identical shapes (for MCF7 cells), are statistically identical ($p > 0.05$). Corresponding columns which have different letters or different shapes are statistically different ($p < 0.001$).

Bcl-2-associated X (BAX) genes, and induce apoptosis via the Bcl-2 family of proteins (Wang et al. 2013). Researchers have also concluded that gold nanoparticles enhance the production of ROS (Geng et al. 2011) and low energy electrons (Chow et al. 2012), which attack cancerous cells and enhance radiotoxicity.

Although the radiation dose was relatively high (2 Gy), MTT assay showed that the cell viability percentage of irradiated MCF7 cells (X-ray group) was not different from the control groups ($p > 0.05$, Figures 3(A) and 5(A)). On the other hand, results of the colony assay performed after 10–14 days showed a decreased cell survival fraction for this group ($p < 0.001$, Figures 3(B) and 5(B)); this indicates that in spite of the MTT test result, MCF7 cells were significantly affected by 2 Gy irradiation. This discrepancy may be linked to a tardiness of precocious death (apoptosis) which is induced by radiation in MCF7 cells (Essmann et al. 2004). In order to survey the correctness of this interpretation, the MTT test was repeatedly performed after 96 and 144 h, and the role of time duration between irradiation and cell viability measurement was investigated. New results revealed a significant decrease in cell viability percentage in the X-ray group (Figure 4). Thus, it may be suggested that irradiated MCF7 cells entered the apoptosis phase later than 48 h. Consistent with our results, Janicke et al. observed that irradiated Hela cells entered apoptosis 1 day after irradiation, whereas irradiated MCF7 cells deferred apoptosis for 4 days (Janicke et al. 2001). Although decrease in cell viability was not observed in the X-ray group after 48 h, there was a significant cell viability decrease in Glu-GNP + X-ray group at the same time ($p < 0.001$, Figures 3(A) and 5(A)). This observation may be interpreted that Glu-G nanoparticles forward precocious death in MCF7 cells.

One major concern regarding treatment of cells with nanoparticles is the ability of the particles to penetrate into the cells. Uptake of nanoparticles by the cells depends on several parameters, e.g. the size, shape and coating surface of the particles. Therefore, considering the importance of these parameters and based on other reports (Chithrani et al. 2006; Zhang et al. 2008; Geng et al. 2014), 16 nm spherical gold nanoparticles coated with thio-glucose were utilized in this study. The nanoparticles were coated with glucose because cancerous cells consume glucose and it increases their ability to absorb nanoparticles. Chithrani et al. (2006) compared spherical, cubic and rod nanoparticles to determine which one is more easily absorbed by the cells. They showed that spherical nanoparticles are taken up more effectively than other shapes. In another study, Glu-G nanoparticles with different sizes (16 and 49 nm) were used to enhance radiotoxicity of megavoltage X-rays in MDA MB 231 cells (Wang et al. 2015). The results showed that 49-nm Glu-G nanoparticles induce stronger radiosensitivity than 16 nm Glu-G nanoparticles with a SER of 1.9 and 1.5, respectively. Nevertheless, in the present study Glu-G nanoparticles were made with the size of 16 nm to be applicable in continuum in vivo studies, since particles with a size of around 50 nm cannot penetrate into blood vessels (Geng et al. 2014). The results revealed that the model of Glu-G nanoparticles made in this study was appropriate, since they were absorbed by the cells effectively.

Although our results revealed the nanoparticles utilized in this study are appropriate and sufficiently penetrate into the cultured cells, there are other issues which must be considered in the case of in vivo tumors; especially when they are not subcutaneous and cannot receive nanoparticles directly by injection. To target tumors and exclude normal tissues, nanoparticles are mostly bound to specific biomolecules which are found and captured by their complementary molecules on the cancerous cells' membrane. Binding nanoparticles with these biomolecules enlarges their size, and may decrease their permeability into blood vessels. On the other hand, in some cases it is appropriate to synthesize large nanoparticles to prevent their penetration into normal tissues; since some studies have shown tumor vessels have higher permeability to large particles compared to normal blood vessels. According to Jain et al. study the vessel-wall structure in tumors is abnormal (Jain et al. 2014). The tumors' vessels have wide interendothelial junctions, an abnormally thick or thin basement membrane, large number of fenestrated channels, and maximum pore diameters as large as several hundred nanometers (Mirkin and Niemeyer 2007). The authors believe that remodeling of intermediate-sized nanoparticles (20–40 nm) can also benefit from tumor vasculature, and tumor vessels can enhance the transvascular delivery of intermediate-size nanoparticles of up to 40 nm. Moreover, smaller nanoparticles experience a significantly lesser degree of diffusional hindrance, resulting in a more homogeneous distribution within the tumor interstitium. Jiang et al. demonstrated that there is a two-stage transport strategy for different size nanoparticles (Jiang et al. 2015). Based on this debate, by employing the results obtained in the current study and other investigations, it is necessary to plan in vivo studies and examine the efficacy of the same nanoparticles in animal models. This is particularly true in the case of high energy X-rays, since they are used to treat deep tumors which can receive nanoparticles only through blood vessels. In this case, it is appropriate to add proper biomolecules to the nanoparticles, measure their penetration into tumors and normal tissues, and determine their efficacy for increasing the therapeutic ratio.

Conclusion

It was demonstrated that Glu-G nanoparticles have remarkable potential to enhance radiotoxicity of both low and high energy photons in MCF7 and QU-DB cancerous cells. It may also be concluded that Glu-G nanoparticles forward apoptosis in irradiated MCF7 cells which defer apoptosis for 4 days. The size, shape and surface coating of the gold nanoparticles designed and made in this study were appropriate, as they resulted in a higher uptake of particles, with no cytotoxicity in either cell lines. Since radiotoxicity enhancement of megavoltage photons by Glu-G nanoparticles was confirmed, it is recommended to continue such work in animal models along with modifying gold nanoparticles to maintain their targeting ability and stability in clinical practice. In addition, since high atomic number nanoparticles may not increase the physical radiation dose, due to the domination of the Compton effect, it is necessary to investigate the mechanisms underlying cell radiosensitization.

Acknowledgements

This paper was extracted from an MSc thesis of Medical Physics. The authors would like to thank Dr Neda Attaran-Kakhki and Sara Mohammadi for their kind cooperation in this research as well as the Research Deputy of MUMS for financial support of this project, numbered (911095).

Disclosure statement

The authors report no conflict of interest. The authors alone are responsible for the content and writing of the paper.

References

Bhattacharyya S, Kudgus RA, Bhattacharya R, Mukherjee P. 2011. Inorganic nanoparticles in cancer therapy. Pharm Res. 28:237–259.

Butterworth KT, Coulter J, Jain S, Forker J, Mcmahon S, Schettino G, Prise K, Currell F, Hirst D. 2010. Evaluation of cytotoxicity and radiation enhancement using 1.9 nm gold particles: potential application for cancer therapy. Nanotechnology. 21:295101.

Chithrani BD, Ghazani AA, Chan WC. 2006. Determining the size and shape dependence of gold nanoparticle uptake into mammalian cells. Nano Lett. 6:662–668.

Cho EC, Au l, Zhang Q, Xia Y. 2010. The effects of size, shape, and surface functional group of gold nanostructures on their adsorption and internalization by cells. Small. 6:517–522.

Chow JC, Leung MK, Fahey S, Chithrani DB, Jaffray DA. 2012. Monte Carlo simulation on low-energy electrons from gold nanoparticle in radiotherapy. J Phys Conf Ser. 341:012012.

Essmann F, Engels IH, Totzke G, Schulze-Osthoff K, Jänicke RU. 2004. Apoptosis resistance of MCF-7 breast carcinoma cells to ionizing radiation is independent of p53 and cell cycle control but caused by the lack of caspase-3 and a caffeine-inhibitable event. Cancer Res. 64:7065–7072.

Evans H Jr. 1994. CRC handbook of chemistry and physics, 75th ed. Vol. 12. Lide DR, editor. Boston: CRC Press; p. 1.

Geng F, Song K, Xing JZ, Yuan C, Yan S, Yang Q, Chen J, Kong B. 2011. Thio-glucose bound gold nanoparticles enhance radio-cytotoxic targeting of ovarian cancer. Nanotechnology. 22:285101.

Geng F, Xing JZ, Chen J, Yang R, Hao Y, Song K, Kong B. 2014. Pegylated glucose gold nanoparticles for improved in-vivo bio-distribution and enhanced radiotherapy on cervical cancer. J Biomed Nanotechnol. 10:1205–1216.

Hainfeld JF, Dilmanian FA, Slatkin DN, Smilowitz HM. 2008. Radiotherapy enhancement with gold nanoparticles. J Pharm Pharmacol. 60:977–985.

Jain S, Hirst D, O'Sullivan J. 2014. Gold nanoparticles as novel agents for cancer therapy. Br J Radiol. 85:101–113.

Janicke R, Engels IH, Dunkern T, Kaina B, Schulze-Osthoff K, Porter AG. 2001. Ionizing radiation but not anticancer drugs causes cell cycle arrest and failure to activate the mitochondrial death pathway in MCF-7 breast carcinoma cells. Oncogene. 20:5043–5053.

Jiang W, Huang Y, An Y, Kim BY. 2015. Remodeling tumor vasculature to enhance delivery of intermediate-sized nanoparticles. ACS Nano. 9:8689–8696.

Kobayashi K, Usami N, Porcel E, Lacombe S, Le Sech C. 2010. Enhancement of radiation effect by heavy elements. Mutat Res. 704:123–131.

Kong T, Zeng J, Wang X, Yang X, Yang J, Mcquarrie S, Mcewan A, Roa W, Chen J, Xing JZ. 2008. Enhancement of radiation cytotoxicity in breast-cancer cells by localized attachment of gold nanoparticles. Small. 4:1537–1543.

Lechtman E, Chattopadhyay N, Cai Z, Mashouf S, Reilly R, Pignol J. 2011. Implications on clinical scenario of gold nanoparticle radiosensitization in regards to photon energy, nanoparticle size, concentration and location. Phys Med Biol. 56:4631.

Malugin A, Ghandehari H. 2010. Cellular uptake and toxicity of gold nanoparticles in prostate cancer cells: a comparative study of rods and spheres. J Appl Toxicol. 30:212–217.

Mesbahi A, Jamali F. 2013. Effect of photon beam energy, gold nanoparticle size and concentration on the dose enhancement in radiation therapy. Bioimpacts. 3:29.

Mirkin CA, Niemeyer CM. 2007. Nanobiotechnology II: more concepts and applications. Weinheim: John Wiley & Sons.

Mohammadi S, Khoei S, Mahdavi SR. 2012. The combination effect of poly (lactic-co-glycolic acid) coated iron oxide nanoparticles as 5-fluorouracil carrier and X-ray on the level of DNA damages in the DU 145 human prostate carcinoma cell line. J Bionanosci. 6:23–27.

Pakravan D, Ghorbani M, Momennezhad M. 2013. Tumor dose enhancement by gold nanoparticles in a 6 MV photon beam: a Monte Carlo study on the size effect of nanoparticles. Nukleonika. 58:275–280.

Rahman WN, Bishara N, Ackerly T, He CF, Jackson P, Wong C, Davidson R, Geso M. 2009. Enhancement of radiation effects by gold nanoparticles for superficial radiation therapy. Nanomedicine. 5:136–142.

Singh NP, McCoy MT, Tice RR, Schneider EL. 1988. A simple technique for quantitation of low levels of DNA damage in individual cells. Exp Cell Res. 175:184–191.

Trono JD, Mizuno K, Yusa N, Matsukawa T, Yokoyama K, Uesaka M. 2011. Size, concentration and incubation time dependence of gold nanoparticle uptake into pancreas cancer cells and its future application to X-ray drug delivery system. JRR. 52:103–109.

Turner J, Koumenis C, Kute TE, Planalp RP, Brechbiel MW, Beardsley D, Cody B, Brown KD, Torti FM, Torti SV. 2005. Tachpyridine, a metal chelator, induces G2 cell-cycle arrest, activates checkpoint kinases, and sensitizes cells to ionizing radiation. Blood. 106:3191–3199.

Van den Heuvel F, Locquet JP, Nuyts S. 2010. Beam energy considerations for gold nanoparticle-enhanced radiation treatment. Phys Med Biol. 55:4509

Wang C, Li X, Wang Y, Liu Z, Fu L, Hu L. 2013. Enhancement of radiation effect and increase of apoptosis in lung cancer cells by thio-glucose-bound gold nanoparticles at megavoltage radiation energies. J Nanopart Res. 15:1–12.

Wang C, Jiang Y, Li X, Hu L. 2015. Thioglucose-bound gold nanoparticles increase the radiosensitivity of a triple-negative breast cancer cell line (MDA-MB-231). Breast Cancer 22:413–420.

Zhang X, Xing JZ, Chen J, Ko L, Amanie J, Gulavita S, Pervez N, Yee D, Moore R, Roa W. 2008. Enhanced radiation sensitivity in prostate cancer by gold nanoparticles. Clin Invest Med. 31:160–167.